Acoustics Loads on Upper-Surface-Blown Powered-Lift Systems

Conrad M. Willis,* James A. Schoenster,* and John S. Mixson†
NASA Langley Research Center, Hampton, Va.

Fluctuating surface pressures were measured in the jet impingement region of upper-surface-blown configurations having rectangular and D-shaped nozzles. Scaling relationships for these fluctuating pressures were studied using models having scale factors of 4-to-1. The scaling relationships generally provided reasonable agreement for the fluctuating-pressure power-spectral-density functions. Effects of forward velocity, jet impingement angle, and angle of attack were small over the parameter range investigated.

Introduction

AIRCRAFT currently under development for STOL application, for example the YC-14 and YC-15, utilize powered-lift concepts that result in large areas of the aircraft surface being immersed in the turbulent flow of the jet exhaust. One of these concepts, upper surface blowing (USB), places the jet exit just above the upper surface of the wing to produce powered lift from the jet exhaust blowing over the deflected flap. This direct impingement of the jet produces a significant increase in the fluctuating pressure loads and must be considered in the structural design of the aircraft.

A Langley Research Center program has conducted or sponsored several investigations to define USB fluctuating pressure loads and to develop methods for their prediction in order to allow the incorporation of appropriate structural properties in the early design stages. Some of the results from this program are presented in Refs. 1 through 11. Aerodynamic characteristics were also determined in some of the tests but this paper will consider only fluctuating pressure loads. Five models were tested to provide data for a range of model sizes and configurations. Two nozzle configurations, a D-shape and a rectangular shape, were investigated. Test parameters were jet velocity, wind tunnel freestream velocity, angle of attack, vortex generator deployment, and jet impingement angle. Overall levels of fluctuating pressures and power spectra for selected conditions were previously presented[1-3] for all five models and scaled spectra were presented[3] for the rectangular nozzle model.

This paper presents new data from the same program to show the effects of the test parameters of airspeed, angle of attack, and angle of jet impingement not evaluated in the previous papers. Scaling relationships are examined to show their applicability for extrapolating data to a different model size and some of the reference data are used to make comparisons. In addition, the measurement locations required to define the load are examined.

Models

A brief description of the five models tested is given in Table 1 and model photographs are presented in Figs. 1 and 2. The models range in size from a nozzle width of 290 cm for model 1 to 4.2 cm for model 5. Two nozzle configurations were used, a D-shaped nozzle for models 1 and 2, and a rectangular nozzle for models 3, 4, and 5. Model 3 is a wind tunnel model and replicates a whole aircraft; the other models were used for static tests and replicate only the areas adjacent to the engine exit.

Model 1 is a full-scale model[2] of the flaps, engine nacelle, and a portion of the fuselage sidewall of a YC-14 STOL transport.[9] The CF6-50D turbofan engine with a D-shaped nozzle and the flaps are flight hardware, while the fuselage and wing are of a boilerplate construction. Model 2 (Fig. 1) is a ¼-scale model[4,5] of the YC-14 nozzle, flaps, and fuselage sidewall and uses a JT15D-1 engine. Model 3 (Fig. 2) is a twin-engine Aero Commander aircraft[6] with the tail removed and the wing and engines modified to represent a USB configuration. The engines were JT15D-1 turbofans with rectangular nozzles. Model 4 is the same shape and scale[7] as model 3 and uses the same engine, but replicates only the flap upper surface. Model 5 is a ¼-scale replica of model 4 flap and nozzle geometry[3,8] but uses a cold-air jet to represent the jet engine.

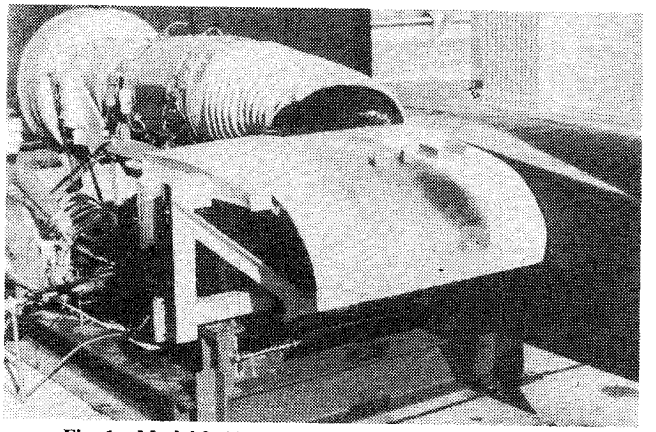

Fig. 1 Model 2, ¼-scale YC-14 flaps, D-shaped nozzle.

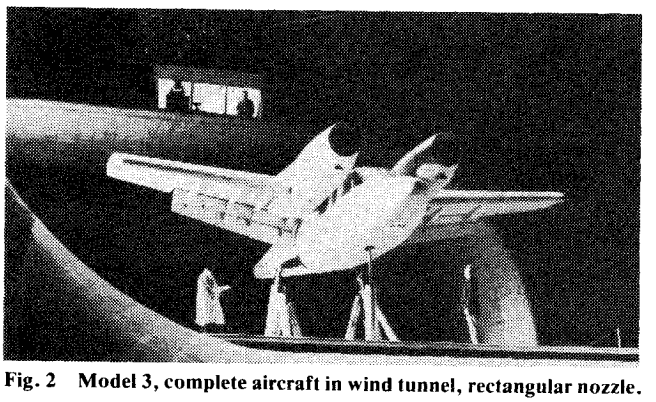

Fig. 2 Model 3, complete aircraft in wind tunnel, rectangular nozzle.

Presented as Paper 77-1363 at the 4th AIAA Aero-Acoustics Conference, Atlanta, Ga., Oct. 3-5, 1977; submitted Oct. 26, 1977; revision received June 1, 1978.

Index categories: Jets, Wakes, and Viscid-Inviscid Flow Interactions; Aeroacoustics.

*Aero-Space Technologist. Member AIAA.
†Aero-Space Technologist.

Table 1 Model description and test conditions

	Model 1	Model 2	Model 3	Model 4	Model 5
Description	D-shaped nozzle on full-scale YC-14 flap	D-shaped nozzle on ¼-scale YC-14 flap	Rectangular nozzle on complete aircraft	Rectangular nozzle on flap	Rectangular nozzle on flap
Nozzle size, cm	290 wide	72 wide	16×94	16×94	4.2×23
Engine	CF-6 turbofan	JT15D-1 turbofan	JT15D-1 turbofan	JT15D-1 turbofan	Cold-air jet
Bypass ratio	4.4	3	3	3	0
Thrust, kN	Not avail.	2.33 to 7.68	1.27 to 5.59	1.07 to 6.72	0.004
Jet Mach number, M_j	Not avail.	0.36 to 0.62	0.26 to 0.56	0.21 to 0.56	0.065
Jet vel. V_j, m/s	160	138 to 253	123 to 292	96 to 281	22
Airspeed, V_∞, m/s	0	0	0 and 16	0	0
Test facility	Static (Boeing)	Static (NASA)	Wind tunnel (NASA)	Static (NASA)	Static (UVA)
Reference	1,2	1,4,5	1,6	1,7,13	1,3,8

The CF6-50D engine used for model 1 was rated at 220-kN thrust and was operated at a bypass ratio of 4.4. The JT15D-1 engine used for models 2, 3, and 4 was rated at 10-kN thrust and was operated at a bypass ratio of about 3. The relative position of the primary and secondary nozzles for models 3 and 4 is indicated in Fig. 3. Model 5, the small cold-air jet model did not use bypass flow.

The two nozzle shapes used in this test program are illustrated in Fig. 4. Both configurations have the lower edge of the nozzle flush with the flap upper surface. The effective nozzle area, calculated from nozzle exit velocity and mass flow, is about 7% less for the model 2 D-shaped nozzle than that for the model 4 rectangular nozzle. Since the areas are about the same and the nozzles were mounted on the same engine, any differences in loads near the exit for models 2 and 4 are due to nozzle shape. The model 2 D-shaped nozzle had a width of 0.72 m for the basic nozzle; this test was conducted with the nozzle side door open which increases the effective width. The rectangular nozzle for model 4 is 0.94 m wide and has an aspect ratio of 6. The same nozzle was used for models 3 and 4. A deflector along the upper edge of the nozzle increased the impingement angle of the jet exhaust on the flap surface.

The shape and relative size of the flaps for models 2 and 4 is compared in the right half of Fig. 4. Flap deflection, defined as the angle between tangents to the flap upper surface at the trailing edge and at the jet exit was 74 deg for the rectangular nozzle and 87 deg for the D-shaped nozzle model. The run length, measured along the flap upper surface from the jet exit to the trailing edge, was 1.6 m for the D-shaped nozzle model 2 and 2.1 m for the rectangular nozzle model 4. The jet impingement angle, as defined for this paper, is the angle between a tangent to the flap upper surface at the jet exit and the direction assumed by the jet thrust vector with the wing removed. The impingement angle is about 5 deg for models 3 and 5. The impingement angle for model 4 is adjustable by rotating the flap about an axis along the lower edge of the nozzle. The impingement angle was not measured for the D-shaped nozzle models. The D-shaped nozzle models are equipped with vortex generators consisting of four small flat plates that extend perpendicular to the flap surface when the flaps are deflected to the landing configuration and retract flush with the surface for all other flight conditions. The measurement locations for the fluctuating pressure loads on the flap are indicated by black dots in Fig. 5.

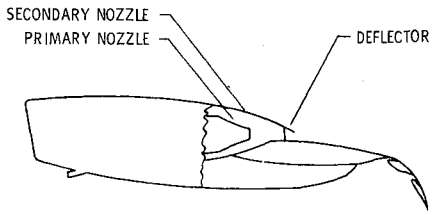

Fig. 3 Sketch of engine and wing, model 3.

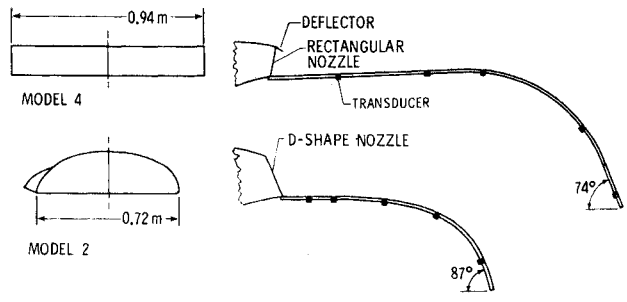

Fig. 4 Nozzle and flap profiles.

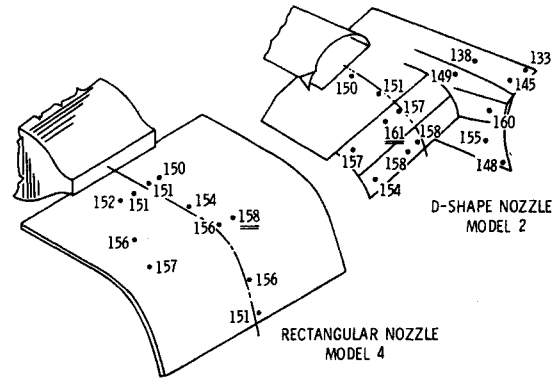

Fig. 5 Distribution of fluctuating pressure loads, OAFPL dB, $M_j = 0.56$.

Tests

Fluctuating pressure loads on aerodynamic surfaces in or near the jet impingement region were measured for all five models. The data were recorded on magnetic tape for later analysis. Test conditions for the data presented herein are summarized in Table 1. The three models (2, 3, and 4) using the JT15D engine were tested by Langley Research Center, the ¼-scale cold-air rectangular nozzle was tested by the University of Virginia, and the full-size YC-14 was tested by The Boeing Company. Model 4 was tested in an inverted position to avoid possible ground effects on the aerodynamic data obtained in the same test program and presented in a previous paper.[7] Model 2 was tested in an upright position at two elevations, the lowest representing the wing height above the runway for the taxi condition. Comparison of the data indicated little or no effect of ground proximity on fluctuating pressure level for the height range of this test. Test parameters varied in the investigation were: jet velocity, wind tunnel freestream velocity, angle of attack, jet impingement angle, deployment of vortex generators, and model size. Test conditions for all five models are given in Table 1. The range of variables listed in the table is the range for data presented in this paper. Thrust for models 2, 3, and 4 was measured by a strain-gauge balance and thrust for model 5 was calculated. Models 1, 2, and 4 were tested on outside test stands.

Overall Loads

Magnitude

Fluctuating pressure load distributions for the rectangular nozzle model 4 and the ¼-scale D-shaped nozzle model 2 with vortex generators down are presented in Fig. 5. The highest loading measured for the $M_j = 0.56$ condition presented was an overall fluctuating-pressure level (OAFPL) of 161 dB; this level is well above the minimum level at which acoustic loading should be considered in the design process. References 12 and 13 indicate that fatigue of light secondary structures in conventional aircraft may become a problem when the OAFPL loading exceeds 130 dB. The turbulent boundary layer loading on some areas of the aircraft may exceed this level and require some design attention. For example, Ref. 9 reports flight loadings measured on areas outside the impingement region of the YC-14 STOL transport that were in the 130- to 145-dB range for a cruise Mach number of 0.7. Since the impingement region loading is substantially higher than the background loading of the trubulent boundary layer, use of a USB configuration will require a more complex design for the impingement region structure. This configuration will also require more attention to noise reduction procedures to provide an acceptable interior noise level for the crew and passengers.

Distribution

The load distributions shown in Fig. 5 indicate the D-shaped nozzle produces loads a few dB higher than the rectangular nozzle, but the rectangular nozzle is wider and, therefore, loads a wider area of the wing. The loading is significant over the entire area immersed in the jet efflux, which includes much of the flap and some of the fuselage sidewall. Both configurations experience the highest loads near the knee of the flap. The jet-exhaust temperatures for model 2 are near those for the full-scale aircraft (model 1) and the measured overall levels of fluctuating pressure for a given measurement location and jet velocity agree well with full-scale measurements.[10] Therefore, the loadings shown in Fig. 5 are considered representative of USB aircraft.

The chordwise distribution of loading across the flap at the nozzle centerline for the rectangular and D-shaped nozzles is shown for two jet Mach numbers in Fig. 6. The shapes of the plots forward of the knee and the levels of the loads are similar and, as previously noted, the highest loads are near the knee of the flap. However, the differences in the geometry of

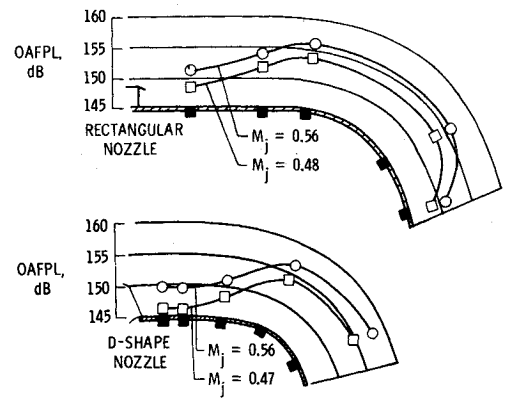

Fig. 6 Chordwise distribution of flap loads at nozzle centerline, $M_\infty = 0$.

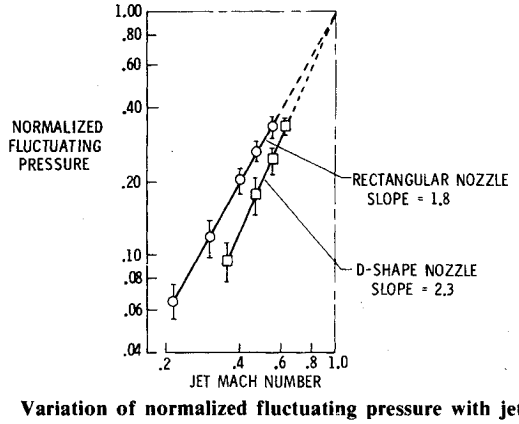

Fig. 7 Variation of normalized fluctuating pressure with jet Mach number.

the two models does produce some difference in loading aft of the knee. The decrease in load at the trailing edge which occurs with the rectangular but not the D-shaped nozzle may be due to the longer flap used with the rectangular nozzle.

Selection of Measurement Locations

It is important to select a transducer location pattern that gives adequate definition to the extent of the high loads of the impingement region. The wide distribution of high loadings shown in Fig. 5 suggests that the region of significant loading may extend beyond the outermost measurement locations. The seven fuselage measurement locations used for the D-shaped nozzle in Fig. 5 appear to define the extent of fuselage loads reasonably well. Both models need additional spanwise locations on the flap, and this would require extension of the model for model 2. The data in Fig. 5 indicate that the selected chordwise locations for the rectangular nozzle were satisfactory but the D-shaped nozzle needed an additional measurement near the trailing edge.

Effect of Jet Mach Number

At a given location, the fluctuating pressure loading increases with jet exit Mach number according to $P = aM^n$ as indicated in Fig. 7. The pressure has been normalized by dividing each pressure by the value of the coefficient, a, which is equal to the value of the pressure, P, at $M = 1.0$, obtained by extrapolating the experimental data for the particular measurement location. This procedure removes the effect of local load level and permits a more convenient comparison of the range of slope for each model. The bars on the plot represent the range of normalized fluctuating pressure for five transducers. The average slope for the D-shaped nozzle was about 0.5 higher than that for the rectangular nozzle. A previous paper[11] noted that USB configurations exhibit a variation of slope with location. No systematic variation of

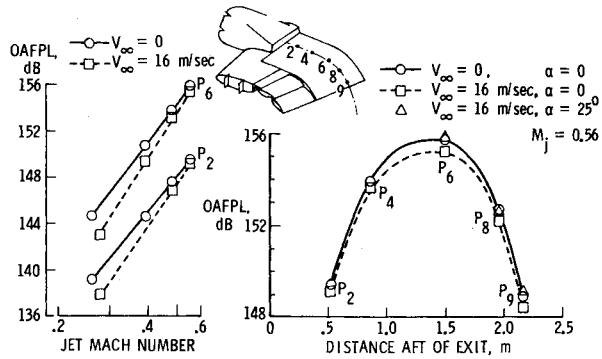

Fig. 8 Effect of airspeed and angle of attack on fluctuating pressure loads.

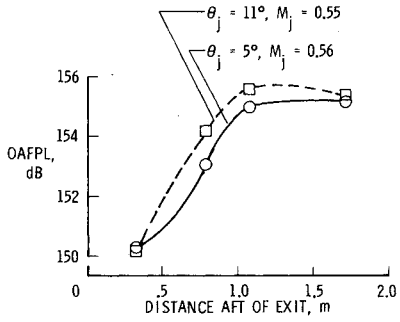

Fig. 9 Effect of jet impingement angle, rectangular nozzle, model 4.

the slope with distance from the exit could be detected in the present test. Since the same engine was used for both sets of data on Fig. 7 and the range of slope variation, indicated by the bars, is about the same for each of the two models, this range of slope is possibly associated with a range of local Mach number due to imperfect mixing of the primary and bypass flows of this engine. The difference in average slope is assumed to be due to the difference in model geometry. None of the other test variables had as much effect on the loads as jet velocity.

Effect of Airspeed

Fluctuating pressure loadings across the flap chord at the nozzle centerline for freestream velocities of 0 and 16 m/s are compared in Fig. 8. The effect of airspeed was small at the one velocity investigated. For jet Mach numbers of 0.56 and small angles of attack, an airspeed of 16 m/s reduced the OAFPL by about ½ dB over the aft half of the flap, with an even smaller reduction closer to the jet exit. Measurements at the outermost location (see Fig. 5) which is near the edge of impingement region indicated reductions of about 1½ dB due to 16 m/s airspeed. The effect of airspeed increased with decreasing jet velocity. At the lowest jet velocity tested, the airspeed was about 12% of the jet velocity and the fluctuating pressure loads were 2 dB lower than the loads for zero airspeed. Increasing the aircraft angle of attack shielded the jet exhaust from the freestream air and tended to reduce the effect of airspeed. At a 25-deg angle of attack, an airspeed of 16 m/s produced no change in the jet loads.

Effect of Jet Impingement Angle

Most USB configurations direct the jet toward the wing surface at an angle of a few degrees to insure attachment and turning of the flow. A jet impingement angle of 5 deg appeared to produce satisfactory flow turning for the rectangular nozzle and most of the data were obtained for this impingement angle. However, one set of data were recorded with an 11-deg impingement angle to determine the effect on fluctuating-pressure loads. These data are presented in Fig. 9.

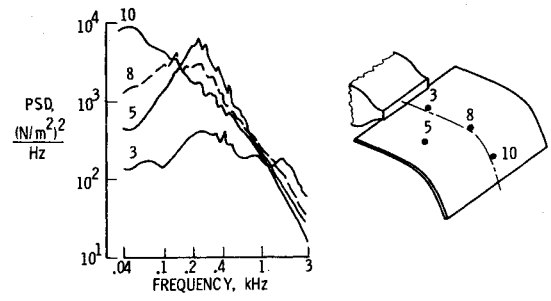

Fig. 10 Fluctuating pressure spectra for rectangular nozzle, model 4, $M_j = 0.56$.

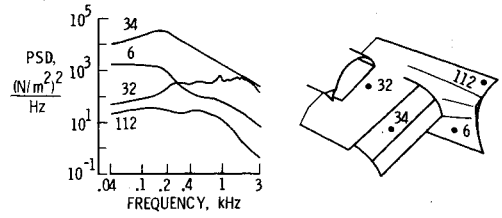

Fig. 11 Fluctuating pressure spectra for D-shaped nozzle, model 2, $M_j = 0.61$.

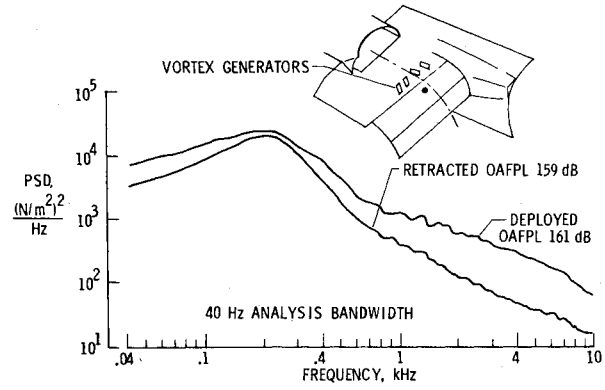

Fig. 12 Effect of vortex generator deployment, model 2, $M_j = 0.62$.

Increasing the impingement angle from 5 deg to 11 deg increased the flap loading along the jet centerline up to about 1 dB at some transducers. The average increase for all transducers was about ½ dB. The effect of impingement angle at a given measurement location was constant over the Mach number range of this test.

Fluctuating Pressure Spectra

Spatial Variation

Some selected spectra for both the D-shaped and rectangular nozzle tests are presented in Figs. 10 and 11. Measurement locations near the jet exit (no. 3, Fig. 10 and No. 32, Fig. 11) and locations outside the impingement region (no. 112, Fig. 11) had spectra that were relatively flat over a wide frequency range. For most of the measurement locations within the impingement region, the power-spectral-density (PSD) maximums occur between 0.04 and 0.25 kHz and then the PSD decreases at about 6 dB per octave. The frequency of the PSD maximum generally decreased with increasing distance aft of the jet exit. Differences in spectra due to variation in airspeed and impingement angle were small at most measurement locations.

Effect of Vortex Generators

The D-shaped nozzle, models 1 and 2, has retractable vortex generators used to improve flow attachment. Figure 12 shows the effect of vortex generator deployment on the

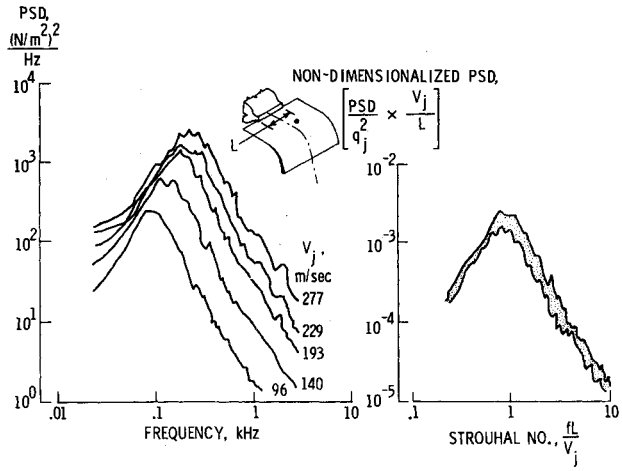

Fig. 13 Comparison of fluctuating pressure PSD for a range of jet velocity, model 4.

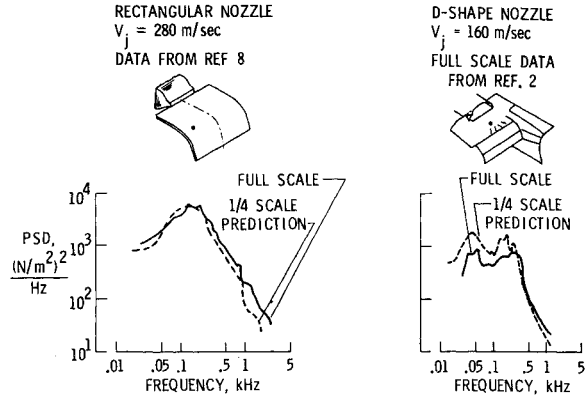

Fig. 14 Comparison of fluctuating pressure spectra predicted from ¼-scale model data with measured spectra from full-scale models.

spectral shape of the fluctuating pressure at one flap location. Most of the change appears to be in the form of an increase in the high-frequency content or decreased rolloff rate. The vortex generators also produced a slight increase of about 1 or 2 dB in the overall acoustic loading. This increase occurred at most of the transducer locations including the ones forward of the vortex generators and those outside the jet flow on the fuselage.

Effect of Jet Velocity

The spectra for five values of rectangular nozzle jet exit velocity are compared on the left side of Fig. 13. The spectrum shape appears to be about the same for all five values of jet velocity, V_j. Spectrum level and the frequency at which maximum amplitude occur both increase with velocity. The right half of Fig. 13 demonstrates the collapse of the same set of data when the frequency and amplitude scales are nondimensionalized. The frequencies were reduced to nondimensional Strouhal numbers by multiplying by L/V_j where the characteristic length, L, is the nozzle width and V_j is the velocity of the jet at the nozzle exit. The PSD values were nondimensionalized by multiplication by $V_j/q_j^2 L$ where q_j is the jet dynamic pressure at the nozzle exit. This adjustment produces a good match of the peak frequencies, but slightly overadjusts the amplitude.

Prediction of Spectra

Spectra predicted from ¼-scale model data (models 2 and 5) are compared with measured full-scale spectra (models 1 and 4) in Fig. 14. The model data were scaled by the method described in Ref. 8. The reference paper indicated that spectra from rectangular nozzle models 4 and 5 showed better agreement when the frequency scales of the normalized spectra, (PSD)$(V_j/q_j^2 L)$ vs fL/V_j or Strouhal number, were multiplied by an empirical factor to account for the difference in jet exit temperature for the two tests. The factor selected was $1/T^{0.75}$ where T is the ratio of jet exit to ambient temperature. The collapse of the spectra indicates that the frequency at which a particular phenomenon (e.g., the maximum energy) occurs is proportional to V_j and inversely proportional to the characteristic length, L, and $T^{0.75}$. The magnitude of the PSD function at the frequency at which this particular event occurs will be proportional to q_j^2/V_j and L. Therefore, measured model spectra for one nozzle size, L_m, and set of test conditions, $(q_j^2/V_j)_m$ and $T_m^{0.75}$, can be scaled to spectra for a full-size nozzle having any desired size, L_{fs}, and desired operating conditions, $(q_j^2/V_j)_{fs}$ and $T_{fs}^{0.75}$ by the following equations:

$$\mathrm{PSD}_{fs} = \mathrm{PSD}_m \left(\frac{L_{fs} q_{fs}^2}{V_{fs}}\right)\left(\frac{V_m}{L_m q_m^2}\right)$$

and

$$f_{fs} = f_m \left(\frac{V_{fs}}{L_{fs} T_{fs}^{0.75}}\right)\left(\frac{L_m T_m^{0.75}}{V_m}\right)$$

The subscripts m and fs are used to indicate model and full-scale quantities. Note that L_m/L_{fs} is the model scale factor. Measured jet temperatures were used in scaling the rectangular nozzle spectrum. Jet temperature for model 1 was not available and the factor $(T_m/T_{fs})^{0.75}$ was assigned a value of 1.0 because the difference in temperature measured in the flap boundary layer of models 1 and 2 was small at a given velocity.

Both of the predicted spectra presented in Fig. 14 are considered to be accurate enough in amplitude and frequency to provide useful information to the aircraft designer. Measurement location for the spectra is indicated by the dots on the sketches. Reference 8 presents predicted spectra for several additional locations.

Conclusions

Fluctuating surface pressure loads have been measured in the jet impingement region on several models of upper-surface-blown flaps. The effects of a number of test parameters were examined and full-scale spectra were predicted from model data. The results have led to the following conclusions.

1) Scale models appear to be an effective means for obtaining fluctuating pressure spectra for use in aircraft design.

2) The effects of airspeed and jet impingement angle on fluctuating pressure loads are small for the 0 to 16 m/s airspeeds and 5 deg to 11 deg impingement angles covered by this investigation.

3) Prediction of full-scale loads from model data will require closely spaced measurement locations.

References

[1] Schoenster, J.A., Willis, C.M., Schroeder, J.C., and Mixson, J.S., "Acoustic-Loads Research for Powered-Lift Configurations," *Powered-Lift Aerodynamics and Acoustics,* NASA SP-406, 1976, pp. 429-433.

[2] Sussman, M.B., Harkonen, D.L., and Reed, J.B., "USB Environment Measurements Based on Full-Scale Static Engine Ground Tests," AIAA Paper 76-624, Palo Alto, Calif., July 1976.

[3] Morton, J.B., Haviland, J.K., Catalano, G.D., and Herling, W.W., "Investigations of Scaling Laws for Jet Impingement," *Powered-Lift Aerodynamics and Acoustics,* NASA SP-406, 1976, pp. 445-463.

[4] Hassell, J.L. Jr., "Results of Static Tests of a ¼-Scale Model of the Boeing YC-14 Powered-Lift System," *Powered-Lift Aerodynamics and Acoustics,* NASA SP-406, 1976, pp. 45-62.

[5] Pappa, R.S., "Surface Fluctuating Pressure Measurements on a ¼-Scale YC-14 Boilerplate Model," AIAA Paper 77-592, Palo Alto, Calif., June 1977.

[6]Staff of Langley Research Center, "Wind Tunnel Investigation of the Aerodynamic Performance, Steady and Vibratory Loads, Surface Temperatures and Acoustic Characteristics of a Large-Scale Twin-Engine Upper-Surface Blown Jet-Flap Configuration," NASA TN D-8235, Nov. 1976.

[7]Shivers, J.P. and Smith, C.C. Jr., "Static Tests of a Simulated Upper-Surface Blown Jet-Flap Configuration Utilizing a Full-Size Turbofan Engine," NASA TN D-7816, Feb. 1975.

[8]Haviland, J.K. and Herling, W.W., "Modeling Techniques for Jet Impingement," AIAA Paper 77-591, Palo Alto, Calif., June 1977.

[9]Butzel, L.M., Jacobs, L.D., O'Keefe, J.V., and Sussman, M.B., "Cabin Noise Behavior of a USB STOL Transport," AIAA Paper 77-1365, Atlanta, Ga., Oct. 1977.

[10]Mixson, J.S., Mayes, W.H., and Willis, C.M., "Effects of Aircraft Noise on Flight and Ground Structures," *Aircraft Safety and Operating Problems,* NASA SP-416, 1976, pp. 513-525.

[11]Mixson, J.S., Schoenster, J.A., and Willis, C.M., "Fluctuating Pressures on Aircraft Wing and Flap Surfaces Associated With Powered-Lift Systems," *Progress in Astronautics and Aeronautics,* Vol. 45, edited by I.R. Schwartz, AIAA, March 1975, pp. 59-81 (also available as AIAA Paper 75-472 Hampton, Va., March 1975).

[12]Lansing, D.L., Mixson, J.S., Brown, T.J., and Drischler, J.A., "Externally-Blown Flap Dynamic Loads," *STOL Technology,* NASA SP-320, 1972, pp. 131-142.

[13]Campbell, J.P., "Overview of Powered-Lift Technology," *Powered-Lift Aerodynamics and Acoustics,* NASA SP-406, 1976, pp. 1-27.